

Asymmetric Liquid Crystalline Dibenzo[a,h]anthracenes for Organic Semiconductors with High Mobility and Thermal Stability

Yucong Bao,^{#a} Liang Zhang,^{#a} Haoming Wei,^a Bingqiang Cao,^{*b} and Tengzhou Yang^{*a}

^a School of Physics and Physical Engineering, Qufu Normal University, Qufu 273165, Shandong, China.

^b School of Material Science and Engineering, University of Jinan, Jinan 250022, Shandong, China.

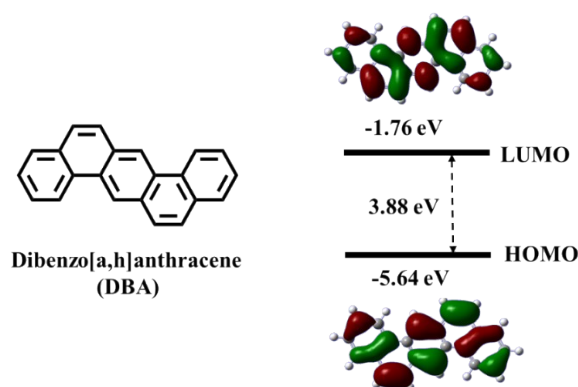


Fig. S1 Calculated frontier molecular orbitals of dibenzo[a,h]anthracene (DBA)

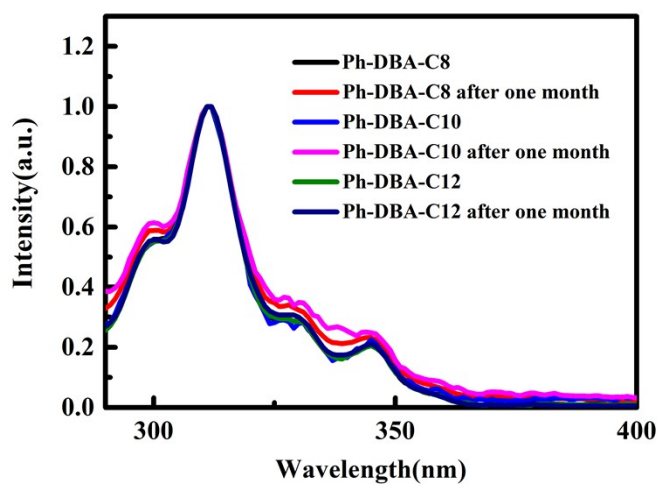


Fig. S2 Time-dependent UV-vis spectra of Ph-DBA-Cn in dilute CHCl_3

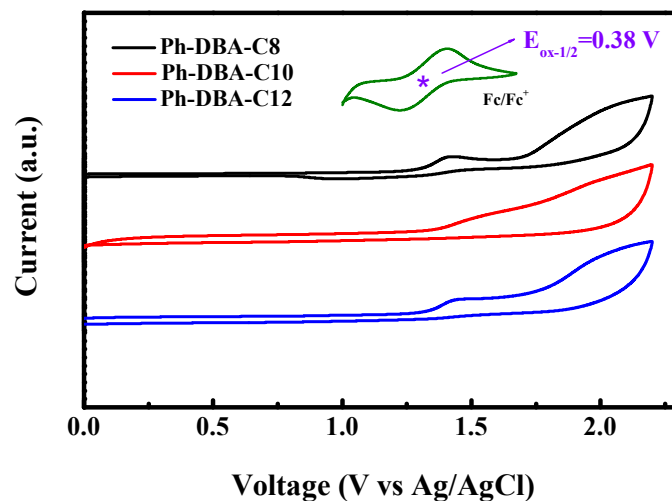


Fig. S3 The CVs of Ph-DBA-Cn in CH_2Cl_2 solution (Cyclic voltammograms measured in 0.1 M tetrabutylammonium hexafluorophosphate solutions with the ferrocene/ferrocenium (Fc/Fc^+) redox couple as the external standard and Ag/AgCl as reference electrode at a scanning ramp of 50 mV s^{-1})

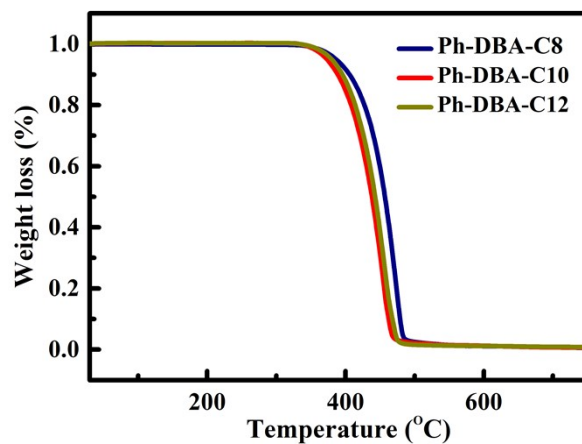


Fig. S4 TGA thermograms of Ph-DBA-Cn at a heating rate of $10 \text{ }^\circ\text{C}/\text{min}$ under N_2 atmosphere

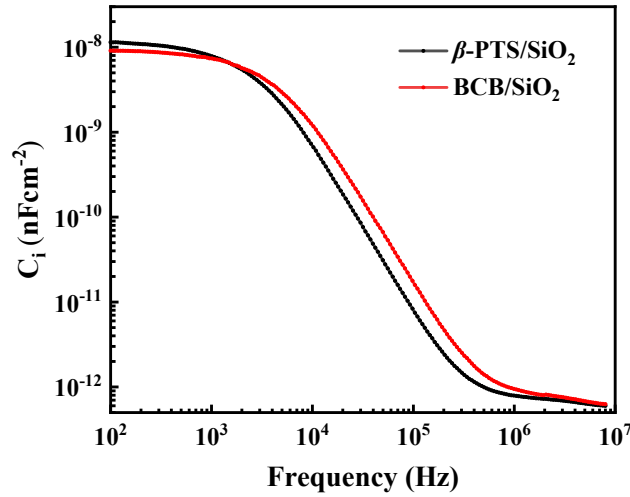


Fig. S5 Frequency dependence of capacitance (C_i) for β -PTS/SiO₂ and BCB/SiO₂ dielectrics measured from the sandwich structure (Au/insulator/heavily p -doped Si), showing C_i of 11.5 and 9.1 nF cm⁻² for β -PTS/SiO₂ and BCB/SiO₂ dielectrics, respectively, at 100 Hz.

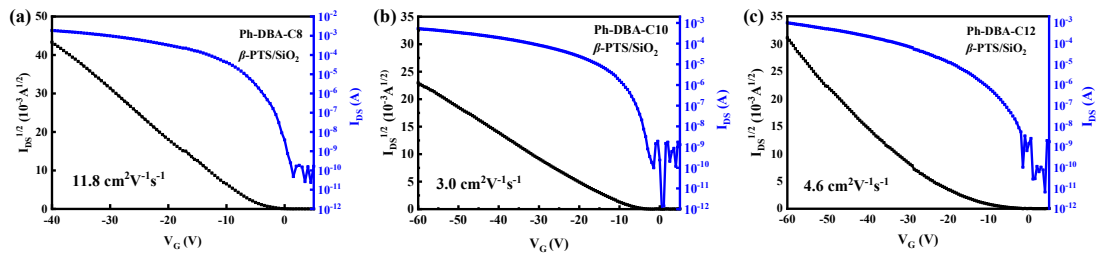


Fig. S6 Transfer curves of Ph-DBA-Cn OTFTs on the β -PTS/SiO₂ dielectric

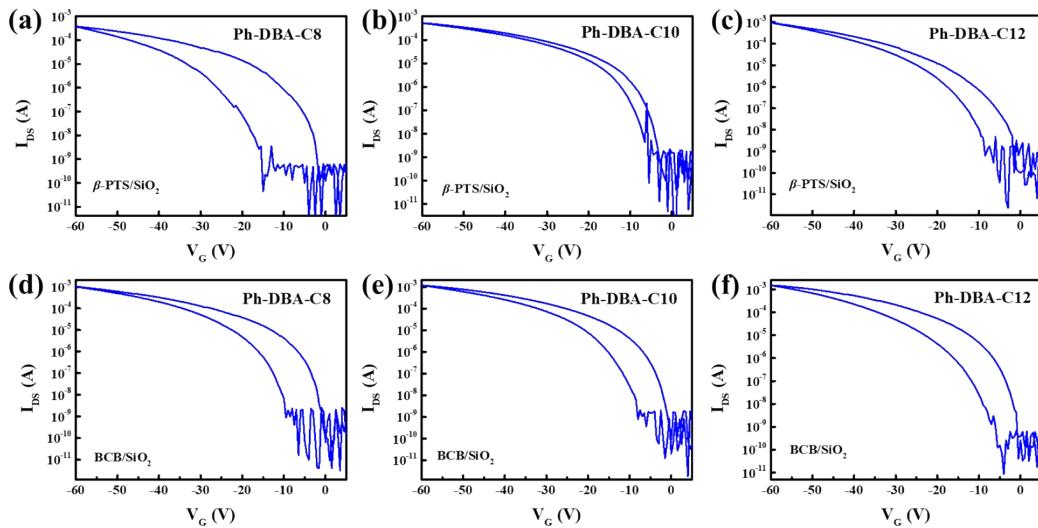


Fig. S7 Transfer curves of Ph-DBA-Cn OTFTs during forward and the forward and reverse scanning

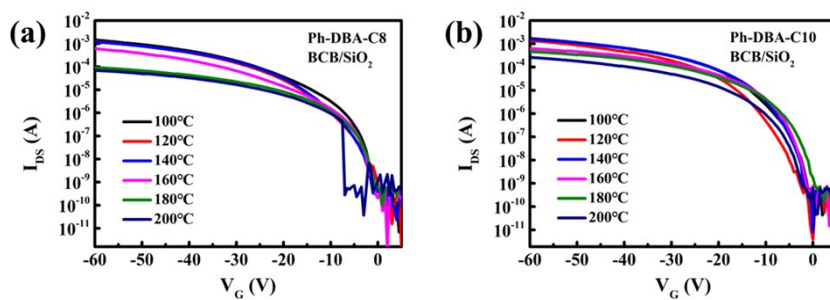


Fig. S8 Temperature-related transfer characteristics OTFTs on the BCB/SiO₂ dielectric (a) Ph-DBA-C8, (b) Ph-DBA-C10

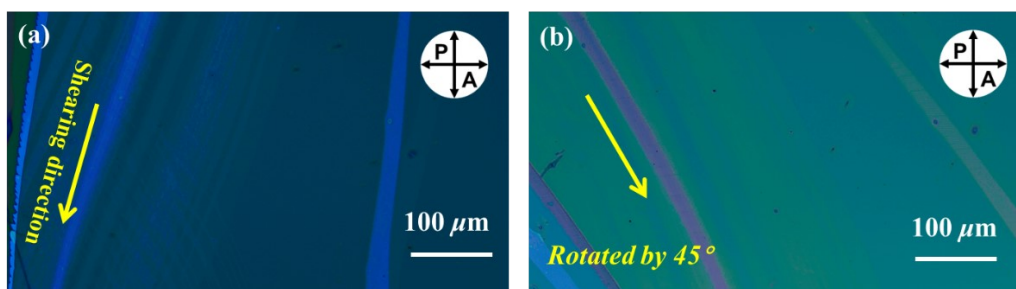


Fig. S9 POM textures of the blade-coated Ph-DBA-C10 film on the BCB-covered substrate (a) 0°, and (b) 45°.

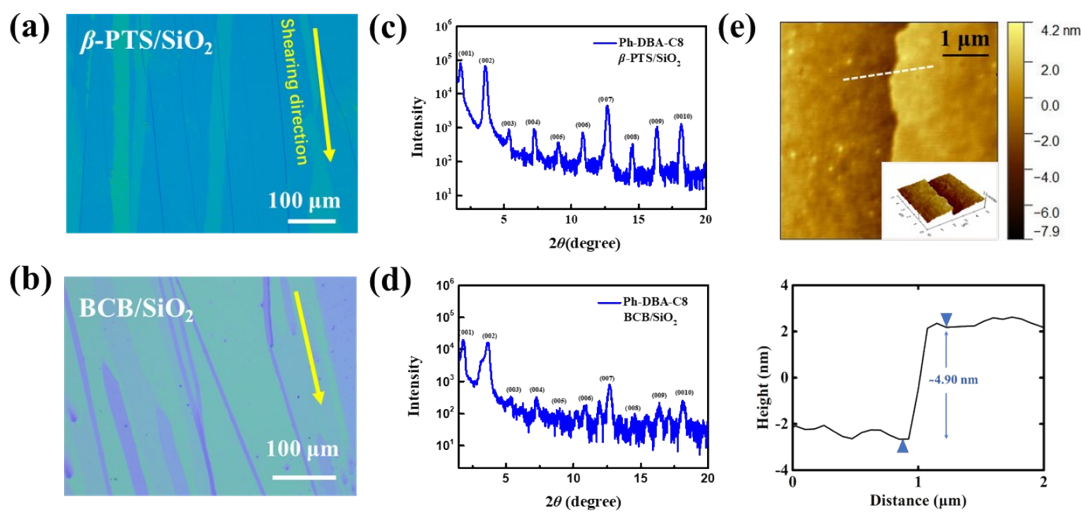


Fig. S10 Optical microscopy images and XRD patterns of the blade-coated Ph-DBA-C8 films on the β -PTS/SiO₂ (a,c) and BCB/SiO₂ (b,d) dielectrics. (e) AFM topographic image and corresponding cross-sectional height profile of the blade-coated Ph-DBA-C8 film on the BCB/SiO₂ dielectric.

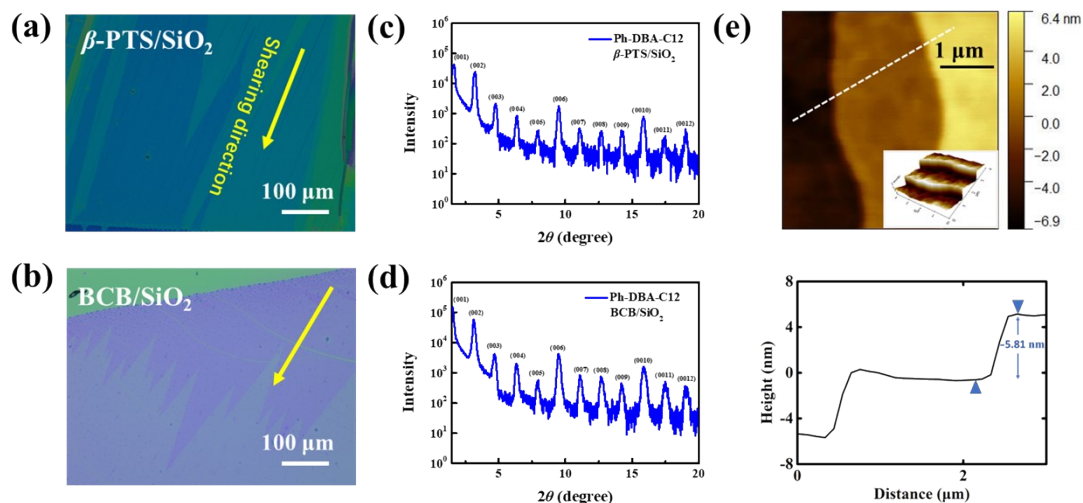


Fig. S11 Optical microscopy images and XRD patterns of the blade-coated Ph-DBA-C12 films on the β -PTS/SiO₂ (a,c) and BCB/SiO₂ (b,d) dielectrics. (e) AFM topographic image and corresponding cross-sectional height profile of the blade-coated Ph-DBA-C12 film on the BCB/SiO₂ dielectric.

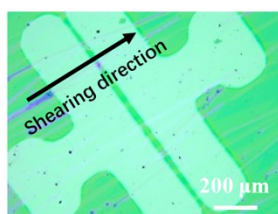


Fig. S12 The optical microscopy image of source/drain electrodes on the blade-coated film

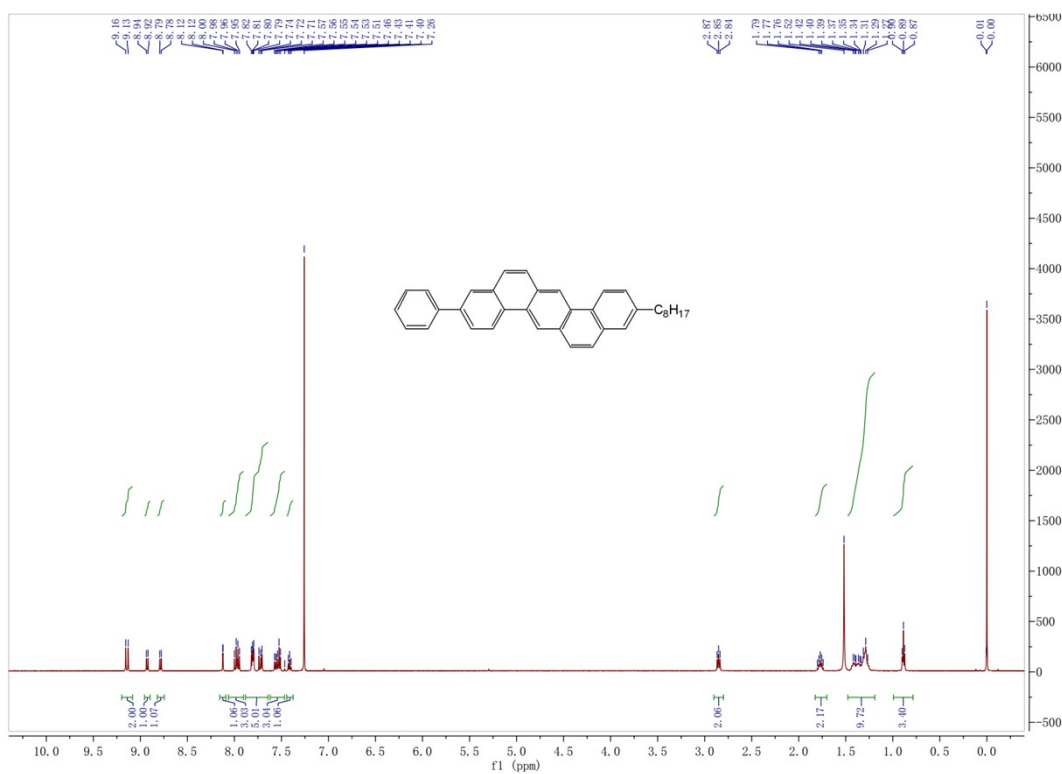
Table S1 Summary of thermal behaviors of phase-transition temperatures ($^{\circ}\text{C}$) with corresponding transitions enthalpies ($\Delta\text{H}/\text{KJmol}^{-1}$) and phases of Ph-DBA-C_n determined by the DSC curves and POM textures during the second heating process at a rate of $10\text{ }^{\circ}\text{C}/\text{min}$.

Compound	Phase Transition T/ $^{\circ}\text{C}$ ($\Delta\text{H}/\text{KJmol}^{-1}$)
Ph-DBA-C8	C _{r1} 131 (-) C _{r2} 207 (0.37) SmE 279 (1.70) SmA 339 (1.28) Iso
Ph-DBA-C10	C _{r1} 129 (-) C _{r2} 197 (0.46) SmE 276 (1.56) SmA 332 (1.20) Iso
Ph-DBA-C12	C _{r1} 121 (0.47) C _{r2} 191 (0.31) SmE 273(1.37) SmA 322 (1.03) Iso
Crystalline: Cr, Smectic: Sm, Isotropic: Iso.	

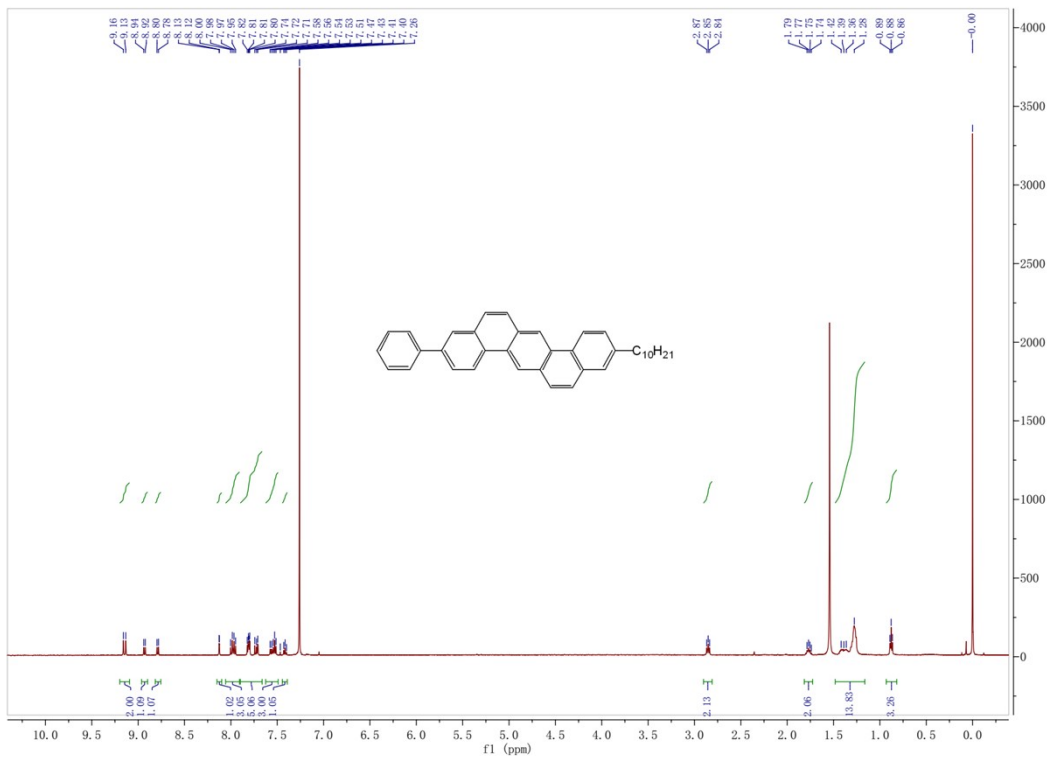
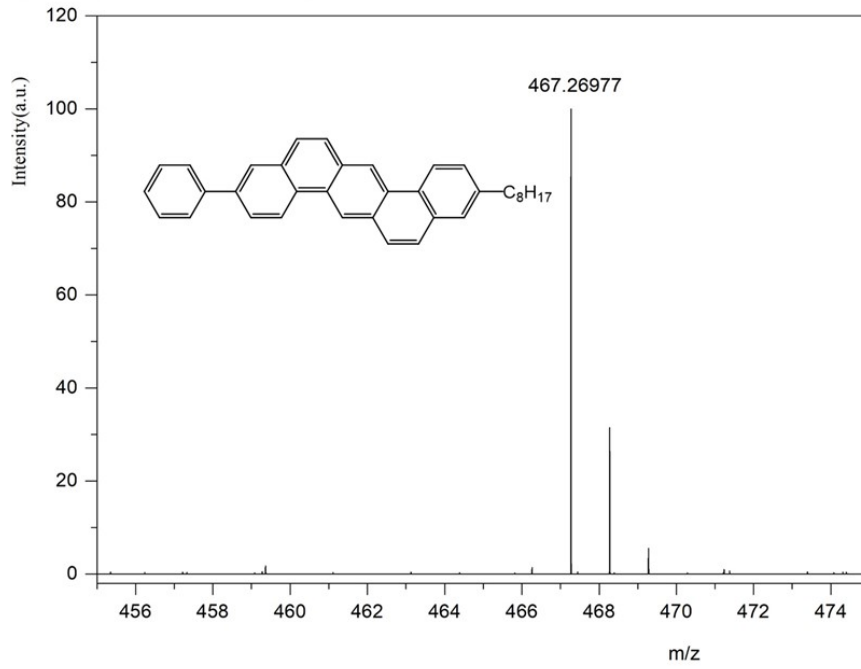
Table S2 Structural parameters of the blade-coated Ph-DBA-Cn films

Compound	Dielectrics	d_{001} (\AA) ^a	L (\AA) ^b	θ_{tilt} ($^\circ$) ^c
Ph-DBA-C8	β -PTS/SiO ₂	50.1	27.2	~23
	BCB/SiO ₂	49.1		~26
Ph-DBA-C10	β -PTS/SiO ₂	50.1	29.4	~32
	BCB/SiO ₂	51.0		~30
Ph-DBA-C12	β -PTS/SiO ₂	52.8	32.3	~35
	BCB/SiO ₂	—		—

^aInterlayer distance determined from the (001) reflection of the XRD patterns. ^bMolecular length estimated from the DFT-Optimized structures. ^cMolecular inclination angle with respect to the substrate normal, defined as $\theta_{\text{tilt}} = \cos^{-1}(d_{001}/2L)$.



CH-1 #9-17_RT: 0.08-0.16_AV: 9_NL:2.41E6
T: FTMS + p APCI corona Full ms [50.0000-750.0000]



CH-1 #9-17_RT: 0.08-0.16_AV: 9_NL:2.41E6

T: _FTMS + p APCI corona Full ms [50.0000-750.0000]

